Journal of Fish Diseases 2016, **39**, 635–647 doi:10.1111/jfd.12383

Comparative imaging of European eels (*Anguilla anguilla*) for the evaluation of swimbladder nematode (*Anguillicoloides crassus*) infestation

K Frisch[1], A Davie[1], T Schwarz[2] and JF Turnbull[1]

1 Institute of Aquaculture, University of Stirling, Stirling, UK

2 Royal (Dick) School of Veterinary Studies, The University of Edinburgh, Roslin Midlothian, UK

Abstract

This study compares diagnostic imaging tools in detecting the parasitic swimbladder nematode *Anguillicoloides crassus* in *Anguilla anguilla* (L.) and focuses on ultrasound in an attempt to develop a non-destructive, field diagnostic test. Ultrasound use could allow the parasite to be diagnosed without decreasing the number of critically endangered European eels through post-mortem. In the preliminary study, eels were examined with computed radiography, computed tomography, magnetic resonance imaging, 14 MHz high-end ultrasound and 5 MHz low-end portable ultrasound, and the results were compared with post-mortem findings. This ultrasound scanning technique did not produce any promising results. A second batch of eels was examined using the same high-end and low-end ultrasounds, but employing a different scanning technique and comparing the results with post-mortem. This second study, scanning along the midline from below, allowed for the detection of anomalies associated with moderately infected animals. None of the eels used in this study were severely infected; thus, no conclusions can be made regarding the use of ultrasound in those animals. Overall, it was found that none of the techniques were useful in diagnosing mildly infected individuals; therefore, no single diagnostic imaging tool is sensitive enough to replace post-mortem for definite diagnosis.

Correspondence *K Frisch, 2568 Byron Road, North Vancouver, BC V7H1M2, Canada (e-mail:* kathleenf@mac.com*)*

Keywords: Anguilla anguilla, *Anguillicoloides crassus*, swimbladder, ultrasound.

Introduction

The European eel, *Anguilla anguilla* (L.), is an ecologically and economically important species throughout Europe (Dekker 2003; Vogel 2010). The market for eels has recently become worldwide; therefore, this species is also globally important (Dekker 2003). The population has been reported to be in steep decline throughout its distributional range during the past decades (Dekker 2003). Stocks are at a historic minimum, with recruitment also being at historically low levels (ICES 2010). As a result, *A. anguilla* has been classified as critically endangered (Vogel 2010; CITES 2011).

According to Dekker (2003), no single hypothesis can be shown to be the cause of the population's rapid decline. This author suggests that a synergetic effect of several causative factors is more likely; these include pollution, habitat loss, climatic changes in the ocean, overexploitation and man-made transfers of diseases and parasites (Moriarty & Dekker 1997). One such parasite is *Anguillicoloides crassus* (Kuwahar, Niimi and Itagaki, 1974), a freshwater nematode of Japanese origin (Taraschewski *et al.* 1987), which has been extensively studied. The parasite was accidentally introduced into Europe in the early 1980s through the importation of infected Japanese eels into Germany (Køie 1991) and was first reported in the UK in 1987 (Kennedy & Fitch 1990). It has spread across Europe and has now become ubiquitous (ICES 2010).

Journal of Fish Diseases

Anguillicoloides crassus adults are found in the swimbladder lumen with the eggs leaving via the pneumatic duct and hatching in the water (De Charleroy *et al.* 1990). Although this is a freshwater parasite, eggs can hatch in a range of salinities and remain infective to intermediate and paratenic hosts (Kirk, Kennedy & Lewis 2000a); however, there is a decline in survival and infectivity as salinity increases. The free-living second-stage larvae are consumed by intermediate hosts, which in Europe include a wide range of freshwater cyclopoid copepods and some estuarine copepods (Kennedy & Fitch 1990; Kirk, Lewis & Kennedy 2000b; Kirk *et al.* 2000a). Once eels consume the infected intermediate host, the larvae penetrate the digestive tract and then migrate across the body cavity and through the swimbladder wall (Haenen *et al.* 1989). In *A. anguilla*, paratenic hosts, which include a wide range of eel food organisms, are a very important part of the life cycle (De Charleroy *et al.* 1990; Thomas & Ollevier 1992; Moravec & Konecny 1994; Székely 1994; Moravec 1996; Moravec & Škoríková 1998). As a result, *A. anguilla* can acquire large numbers of larvae in their body cavities from the paratenic, benthic fish, which form a significant part of their diet, as well as directly consuming the intermediate hosts (Kirk 2003).

According to Kennedy (2007), the rapid spread of *A. crassus* across Europe can be associated with the significant differences in its life cycle compared with that in Pacific eel species. The first is that, in Europe, there is a wider range of intermediate hosts allowing the nematode to complete its life cycle in fresh, estuarine and saline conditions. Secondly, the parasite employs paratenic hosts, which have not been reported in its Pacific life cycle (Nagasawa, Kim & Hirose 1994). This allows young *A. anguilla* to acquire the parasite through ingesting infected copepods and in older and larger eels by ingesting infected fish (Kennedy 2007). Thirdly, it seems that the *A. crassus* larvae take more time to move through the European eel swimbladder wall than in Pacific eels, causing a more intense inflammatory reaction. Compared with Pacific eels, Taraschewski (2006) stated that as a species, *A. anguilla* is an immnuologically naïve host to this parasite and seems unable to mount an effective immune response against it as demonstrated experimentally by Knopf & Mahnke (2004).

Pathological changes caused by *A. crassus* in European eels have been well documented. The parasite causes fibrosis and thickening of the swimbladder wall as well as dilation of the blood vessels and inflammatory and oedematous lesions in the mucosa and submucosa. Granulation occurs around the migrating larvae, and haemorrhages often develop (Molnár *et al.* 1993; Haenen, van Banning & Dekker 1994; Molnár 1994). Previously infected eels will often have a thickened, fibrotic swimbladder wall with intense pigment accumulation and in the most advanced cases the lumen collapses (van Banning & Haenen 1990; Molnár *et al.* 1993). As a result of these pathological changes, the swimbladder becomes dysfunctional. Würtz, Taraschewski & Pelster (1996) showed that there is a reduction in the contribution of oxygen to the swimbladder due to *A. crassus* adults altering the mechanism of gas deposition and therefore, its function as a buoyancy and hydrostatic organ is impeded. The parasite also causes a reduction in swimming ability in laboratory conditions (Sprengel & Lüchtenberg 1991). In addition to the potential for the parasite to survive in eels for up to 6 months in 100% sea water (Kirk *et al.* 2000b), these physiological effects are thought to be partially responsible for the decline in European eels recruitment (Dekker 2003). In other words, it is thought that *A. crassus* infection affects the vertical movements of *A. anguilla* during migration and directly stresses the host throughout the migration to their spawning grounds (Kirk 2003).

Swimbladder disease due to *A. crassus* and other pathogens is difficult to evaluate through external examination and is most commonly detected through post-mortem. Radiography is currently the only non-destructive test for detecting the pathological changes associated with this nematode, which include gas, worm and exudate content of the swimbladder (Beregi *et al.* 1998; Svékely, Molnar & Rácz 2005). This method, however, has been developed as a laboratory-based research tool and is not currently suited for field studies. Computed tomography (CT) has also been used to show gas content, inner structure and wall thickness of eel swimbladders (Székely *et al.* 2004). Székely *et al.* (2004) found that their results correlated well with post-mortem and conventional radiographic findings. To estimate the prevalence of *A. crassus* in river basins, a non-lethal, economically viable, reliable methodology is needed which can be transported and used in the field. Ultrasound could be one such technique.

It has a long history as a diagnostic tool in a wide range of species and has been extensively used for imaging fish, predominantly in determining reproductive status in broodstock management (Martin-Robichaud & Rommens 2001).

The healthy swimbladder is filled with gas, and this tissue–air interface would be a strongly reflective structure to ultrasound. This would cause the sound beam to bounce back and forth between it and the probe, and result in horizontal lines to appear on the image parallel to the real position of the swimbladder wall. These are known as reverberation artefacts (Penninck 2002); they are weaker and are spaced at an equal or a multiple of the distance between the probe and the swimbladder wall (Cartee 1995). Also, when an ultrasound beam encounters media which transmit sound at different velocities – as is the case with gas (an impenetrable barrier to ultrasound) and fluid which offers the least resistance – a proportion of the beam that is not reflected but is transmitted undergoes refraction or bending (Penninck 2002). The nature of the swimbladder structure would produce these artefacts on ultrasonic examination of a healthy individual, meaning that the absence of these would point to an abnormality consistent with the presence of an *A. crassus* infection.

This study investigates the potential use for ultrasound as a portable diagnostic tool in assessing the health state of swimbladders in European eels and comparing these results with those using magnetic resonance imaging (MRI), CT and conventional digital radiography.

Materials and methods

Preliminary imaging study

Five eels were taken to the Royal (Dick) School of Veterinary Studies for diagnostic imaging. Four of these were from the freshwater catchment of the River Thames, which has a high prevalence of *A. crassus*, and one from the Loch Lomond catchment, which was thought to be free of this parasite. The eels were terminally anaesthetized with 300 mg L^{-1} of benzocaine and then placed in individual plastic bags, which were uniquely identified. Using computed radiography (Agfa ADC Solo; Agfa HealthCare UK Ltd), two left lateral views, one cranial and one caudal to cover the entire length of each individual eel, and a dorsoventral view of the cranial half of the fish were taken, the fish being directly placed onto the radiographic cassette.

After radiography, which allowed the eels to be screened for the presence of metal, all five fish were scanned simultaneously using a 1.5 Tesla MRI (Philips Intera, Philips Healthcare, Reigate). CT imaging was then performed on each individual eel using a four-detector-row helical CT scanner (Somatom Volume Zoom, Siemens AG) with the following settings: 120 kVp, 100 mAs, rotation time of 1 s and detector pitch of 1.66. The images were processed into two sets: the first with a reconstructed slice width of 3 mm, a reconstruction increment of 1.5 mm and a soft tissue image reconstruction algorithm (Siemens B40f) and the second with a reconstructed slice width of 1.5 mm, a 0.7 mm reconstruction increment and a bone image reconstruction algorithm (Siemens B70f). After the CT examination, each eel was injected rectally with 5–10 mL of barium sulphate (Baritop® 100; Sanochemia Diagnostics UK Ltd) diluted with water to 5% weight volume^{-1}. The CT imaging was repeated post-barium injection, as well as left lateral and dorsoventral radiographs of the cranial half of each eel.

Following this, the fish were laid in right lateral recumbency with the head to the left and scanned with a harmonic ultrasound (GE Logiq9, General Electric Medical Systems) using a 14 MHz linear transducer for a high-end ultrasonic examination. The area being scanned, between the vent and pectoral fin, was divided up into probe-length sections (5 cm) starting from the vent. Images were taken of each section at the lateral line: first longitudinally and then transversally taking three images per section and labelling them accordingly. This protocol was repeated with a low-end portable ultrasound machine (SonoSite Vet 180plus; FUJIFILM SonoSite Ltd) using a 5 MHz linear transducer.

Once the imaging was completed, each eel's total length and weight were measured and a post-mortem examination was performed. Photographs were taken of the swimbladder *in situ* with all organs except the kidney removed. The swimbladder length was measured and then, this organ dissected out. Photographs were taken of the intact swimbladder and again once opened over its entire length. The swimbladder degenerative index (SDI) developed by Lefebvre, Contournet & Crivelli (2002) was used for each swimbladder. This index is based on scoring three separate

criteria of the gross pathology with 0, 1 or 2 (Table 1), which are then added together to end up with a score out of 6, where 0 is a normal-looking swimbladder and 6 a severely affected one. The length ratio index (LRI), developed by Palstra *et al.* (2007), was also calculated. This index, based on the observation that swimbladders thicken and shorten as a result of subsequent infections, is calculated by dividing the swimbladder length by the total body length. Each swimbladder was then graded out of 5 according to the criteria described by Beregi *et al.* (1998), which can be seen in Table 2, where 1 is an uninfected swimbladder and 5 is a severely affected one.

Post-processing DICOM viewing software (OsiriX version 3.9.2, 32-bit, Open Source™) was used to evaluate all the diagnostic images obtained. A morphological description, as well as swimbladder length, was determined for each set of radiographs, CT, MRI and ultrasonic images.

Ventral ultrasonic imaging study

Following the analysis of the preliminary imaging study results, 14 eels were taken to the Royal (Dick) School of Veterinary Studies for ultrasonic examination; three were from the River Parrett and the 11 from the River Ouse in North Yorkshire. The eels were terminally anaesthetized with 300 mg L^{-1} of benzocaine and uniquely identified. The same two ultrasound machines were used as previously, but the protocol was changed in an attempt to obtain better images. The area being scanned was divided up as previously into sections, but instead of scanning along the lateral line, each eel was individually scanned along the midline from underneath using a plasticized piece of cardboard with a hole in it fitting the size of the transducer.

Following both scans, each eel's weight and length were measured and a post-mortem examination was performed following the same procedure as previously. The SDI, LRI and severity grade of infection were determined for each swimbladder using the same viewing software.

Results

During the preliminary work for this paper, an eel from the Loch Lomond catchment, presumed *A. crassus* free, was found at post-mortem to be mildly infected through the presence of small worms in the swimbladder lumen. This fish was not part of the main imaging study.

Preliminary imaging study

From the four eels from the River Thames, two were mildly infected and the other two moderately infected with *A. crassus*. Only the eel from the Loch Lomond catchment was parasite free. The swimbladder of the eel classified as infection free (fish no. 5) showed a full gas-filled lumen and no evidence of worms on CT (Fig. 1a), radiographic (Fig. 1b) and MRI (Fig. 1c) examinations. The pneumatic duct was gas-filled and could be clearly seen with all three of these diagnostic tools. The high-end and low-end ultrasound examinations showed no observable abnormalities (Fig. 2). There were reverberation artefacts present, and one of the rete mirabile (bundle of closely apposed capillary segments which controls buoyancy by a countercurrent mechanism of gas exchange) was easily identified in the longitudinal view with the high-end ultrasound machine (Fig. 2a1). On post-mortem examination, the swimbladder had a worm-free lumen and a wall that

Table 1 The three criteria of the post-mortem swimbladder degenerative index, each scored 0, 1 or 2 with increasing degradation as developed by Lefebvre *et al.* (2002)

	Score		
Criterion	0	1	2
Transparency/opacity of swimbladder wall	Normal	Partial opacity	Total opacity
Presence of pigmentation and exudate instead of gas in the swimbladder lumen	No pigmentation and no exudate	Either pigmentation or exudate	Both pigmentation and exudate
Thickness of the swimbladder wall	< 1 mm	Between 1 and 3 mm	> 3 mm

Table 2 Severity grades of damage to score the swimbladder health of eels, *A. anguilla*, as a result of infections by the nematode *A. crassus* as described by Beregi *et al.* (1998)

Severity	Post-mortem changes	Radiographic changes
Grade 1	• Swimbladder transparent and thin walled, with the wall thickness not exceeding 0.3 mm • Pneumatic duct not containing gas • Swimbladder collapsing after opening	• Shape of the swimbladder clearly outlined, it gives a homogeneous radiographic shadow under the spinal column, its size is proportional to the body size and usually occupies 15 intervertebral spaces • Wall can hardly be seen or not at all • Sac is divided into 2 parts by the compact substance of the paired gas glands (rete mirabile) or by their shadow
Grade 2	• Swimbladder normally filled with gas • Wall slightly opacified, sometimes containing haemorrhages but not exceeding 1 mm in thickness • Lumen usually containing only a few worms of small size • In some cases, worms also in the lumen of the gas-filled pneumatic duct	• Resembles healthy swimbladder, but middle third is often dilated and ends are tapered • Shadow is non-homogenous • Pneumatic duct is filled with gas, its lumen is distinct and its width often reaches that of the swimbladder • Faintly discernible contours of small-sized worms present in the pneumatic duct or in either end of the swimbladder
Grade 3	• Dilated, gas-filled lumen of the swimbladder containing a small amount of exudates and numerous worms (hollows in the wall) • Dilated lumen of the pneumatic duct often containing worms • Wall opaque and slightly thickened (up to 2 mm but only near the two ends of the sac)	• Radiographic shadow of the swimbladder is deformed and its length equals only that of 12–14 vertebrae • Shadow is of cystic structure due to worms present in the lumen • Pneumatic duct is dilated and contains gas • Contours of worms are often readily discernible both in the swimbladder lumen and in the pneumatic duct
Grade 4	• One or both ends of the swimbladder atrophied, and sometimes one of its halves completely devoid of gas • Lumen containing more or less exudates a few small dead worms • Wall markedly thickened: 2 or 3 mm in the middle third, and even 3–5 mm at the ends • Pneumatic duct looking like an airless bundle	• Narrowed radiographic shadow and its presence is indicated only by a narrowed, occasionally spot-like shadow representing the gas contained by the bladder • Shadow of the pneumatic duct is not visible
Grade 5	• Swimbladder markedly shrunken • Rigid wall containing neither gas nor any other material (exudates, worms), uniformly and markedly thickened, reaching 2-5 mm • Pneumatic duct thin walled, containing no gas	• No gas content can be detected in the swimbladder • Radiographic shadow of the area shows homogenous density corresponding to the abdominal organs

was transparent and thin walled (wall thickness < 1 mm) (Fig. 3).

One of the moderately infected eels (fish no. 1) had a swimbladder that showed contours of worms, a thickened wall and rounded shape of the whole organ on CT (Fig. 4a) and radiographic (Fig. 4b) examination. The MRI images had the same findings, but also showed fluid in the lumen and the caudal end of the swimbladder to be collapsed and fibrotic (Fig. 4c). The high-end and low-end ultrasound examinations showed no observable anomalies (Fig. 5). On post-mortem examination, the swimbladder wall was slightly thickened (1 mm thickness) in the gas-filled

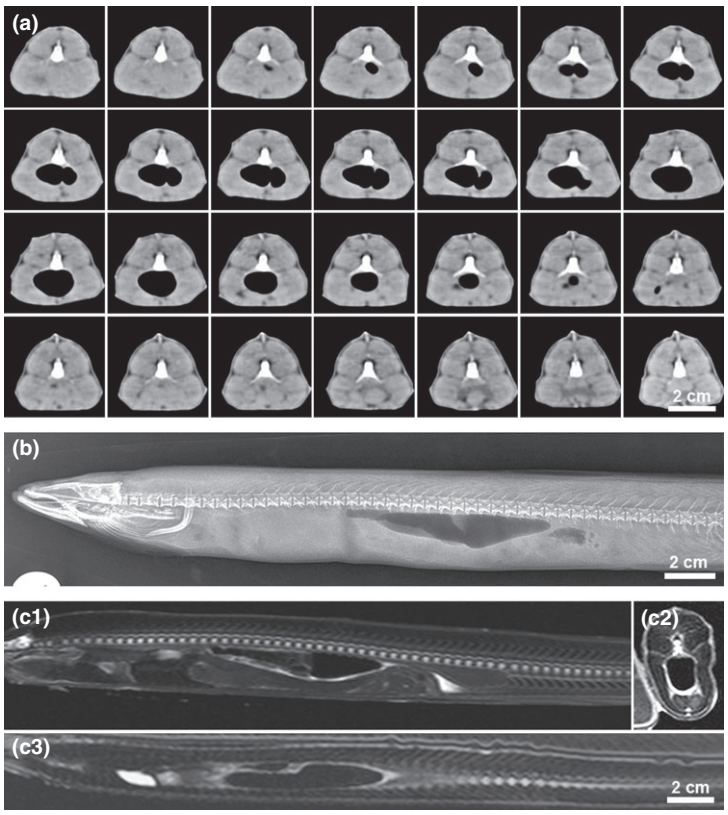

Figure 1 *Anguilla anguilla*, no. 5. (a) Computed tomography showing a clearly discernible parasite-free swimbladder. (b) Lateral radiograph of the cranial half of the same eel with a distinct radiographic shadow of the swimbladder and no visible worms. (c1) Lateral, (c2) transverse and (c3) dorsal T2 MRI images of the same eel showing a clearly visible parasite-free swimbladder in all three views.

section and atrophied at the caudal end. It was also partially opaque and had a small amount of pigmentation throughout. There were large worms and exudate within the lumen (Fig. 6). The other eel with a moderately infected swimbladder (fish no. 2) showed some irregularities on the surface of the swimbladder on the longitudinal view, which could also be seen on the low-end ultrasonic examination. The transverse views did not show these irregularities, but the organ surface in these images was hyper-reflective when compared with the uninfected swimbladder (Fig. 2).

The two eel swimbladders which were classified as mildly infected (fish no. 3 & 4) had similar results. They showed a full gas-filled lumen and no evidence of worms on CT, radiographic or MRI examination. The high-end ultrasonic longitudinal view showed comet tail artefacts (a type of reverberation), but no visible abnormalities in this or the transverse view. No anomalies were found with the low-end ultrasound examination. On post-mortem examination, the swimbladders had thin and transparent walls (wall thickness < 1 mm) with small worms in the lumen.

Table 3 shows the calculated SDI and LRI for each eel, as well as the severity grade of infection based on the criteria in Table 2 for the post-mortem, radiographic, CT and MRI examinations. The ultrasonic examinations were not given a severity grade. The non-infected swimbladder had a SDI of 1 and a severity grade of 1 of 5 on post-mortem. The moderately affected swimbladders had a SDI of 3–4 and a severity grade of 3 of 5. The severity grade of infection for the mildly affected eels was 2 of 5 and the SDI was 1–2. Length could not be measured accurately from the CT or ultrasonic images due to the nature of these tools. LRI ranged from 0.12 to 0.13. Post-mortem measurements of the eels used in the preliminary imaging can be found in Table S1 (fish no. 1–5).

Ventral ultrasonic imaging study

One of the three eels from the River Parrett was mildly infected, and five of the eleven eels from the River Ouse were infected, three moderately and two mildly. SDI, LRI and severity grade of infection for each eel are shown in Table 4. LRI ranged from 0.05 to 0.14 with

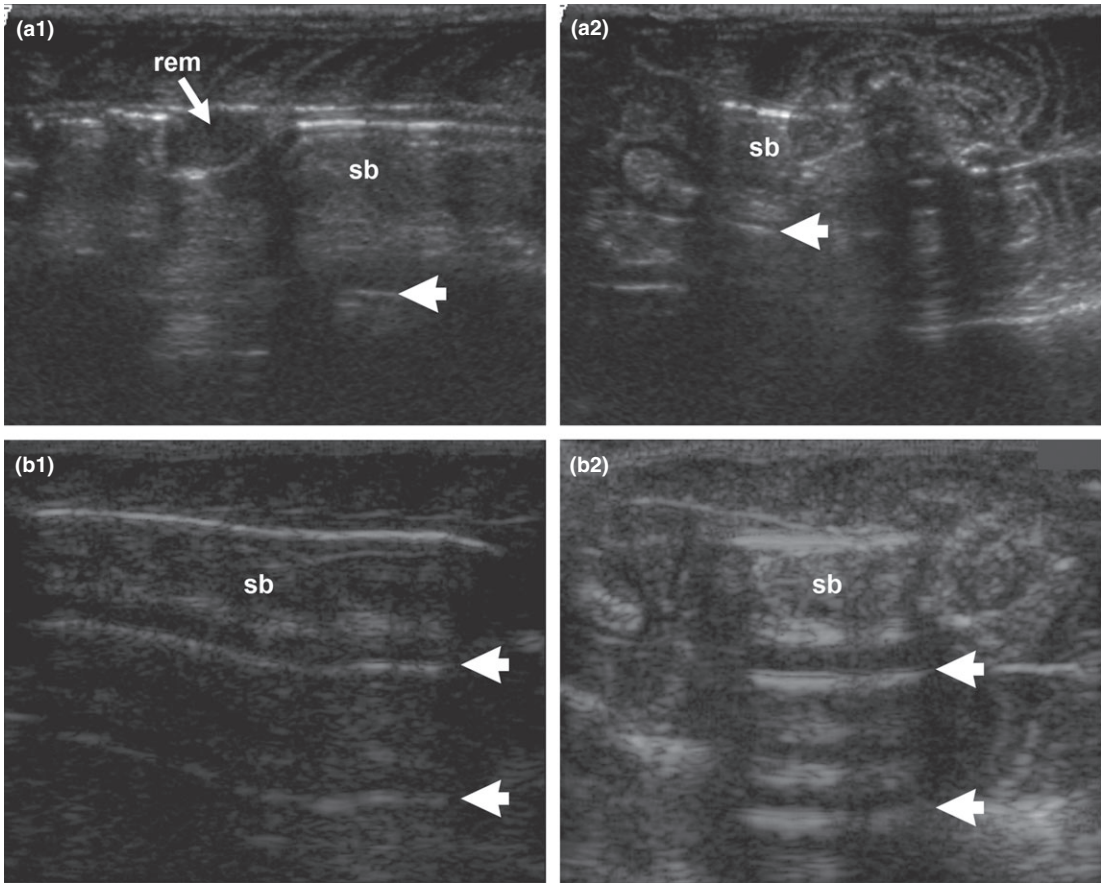

Figure 2 *Anguilla anguilla*, no. 5. (a1) Longitudinal and (a2) transverse high-end ultrasonic images halfway through the swimbladder from eel in Fig. 1 taken with a 14 MHz linear transducer, showing the swimbladder (sb) and the rete mirabile (rem) with reverberation artefacts (short arrows). (b1) Longitudinal and (b2) transverse low-end ultrasonic images of the same swimbladder taken with a 5 MHz linear transducer, showing the swimbladder (sb) with reverberation artefacts (arrow heads).

the lowest numbers not corresponding to the worst swimbladder pathologically. Post-mortem data are shown in Table S1 (fish no. 6–19). Ultrasonic examinations of the non-infected eels did not reveal any anomalies. Reverberation artefacts were present, and the line representing the wall of the swimbladder was smooth and unbroken. The transverse views allowed for the visualization of the pneumatic duct. On post-mortem, these parasite-free swimbladders had walls, which were transparent and thin walled (wall thickness < 1 mm), and the lumen was worm free.

One of the moderately infected eels (fish no. 16) showed irregularities at the caudal end of the swimbladder on both high-end and low-end ultrasound examinations; reverberation artefacts were not seen in this section. These anomalies could be seen in both longitudinal and transverse views. Some undulating movements were observed in that area during the low-end ultrasonic examination. On post-mortem examination, this swimbladder contained two large and seven smaller worms, which were mainly in the caudal end, and the wall was partially opaque and irregular at this end and had pigmentation throughout. Lower degree undulating movements were also seen on one of the mildly infected eels (fish no. 18) during the low-end ultrasound examination. On post-mortem examination, this eel had six small worms in its swimbladder lumen. The other mildly infected eels with less than three worms present in the swimbladder lumen and no significant pathological changes to the swimbladder wall, did not show any visible abnormalities on ultrasonic examination.

Figure 3 *Anguilla anguilla*, no. 5. (a) Unopened and (b) opened swimbladders dissected from eel in Fig. 1. Wall is transparent and thin walled, and lumen is worm free.

Discussion

The results obtained during this study showed that no diagnostic imaging tool alone can provide enough information to be able to sensitively detect *A. crassus* in living eels; therefore, post-mortem examination is still the preferred for definite diagnosis. In the preliminary imaging study, the ultrasound examinations did not show any significant observable changes in the mildly or moderately infected eels when compared with the non-infected one. This was thought to be because the eels were in lateral recumbency and scanned along the lateral line; therefore, the ultrasound beam had to go through the gas-filled section of the organ before reaching any other content in the lumen. The results from the high-end and low-end ultrasounds were similar, although more detail could be seen with the higher frequency probe. It is not known whether a scan of a severely infected eel would show noticeable changes on an ultrasound scan. However, due to the structure of the organ, it is likely that ultrasound could allow the detection of a severely infected eel with a thickened and scarred swimbladder wall as it would contain less gas. Scanning along the ventral midline from underneath, as was performed with the second set of eels, gave more promising results. This method was trialled in view of the fact that if the swimbladder lumen contained exudate or worms, this content would be located at the lowest part of the organ; thus, the ultrasound beam would not have to go through gas before reaching it. From the results, swimbladders that had multiple (> 5) or larger worms had sections where reverberation artefacts were absent, which correlated with worm presence. Also, if the examiner kept the probe still, undulating movements could be seen. Although this second method of scanning produced better results for identifying moderately infected eels, it was still unable to differentiate between mild and parasite-free eels. Another problem encountered was that when the swimbladder wall did not show up as a smooth unbroken line on the images, it was unknown whether this was due to an abnormality or whether the beam was hitting something else such as the side of the organ or the pneumatic duct. The rete mirabile was easily distinguishable as blood filled. Ultrasound imaging can be fast, suggesting it is readily applicable for anaesthetized eels without the risks associated with prolonged examination periods. However, this study's results suggest that ultrasound is not an ideal tool for detecting this type of infection, particularly in mild cases.

The radiographic and CT examinations provided similar information about swimbladder infection status. CT is able to provide more information about the internal structure, gas content and wall thickness of the swimbladder when compared to radiography, which correlates with what

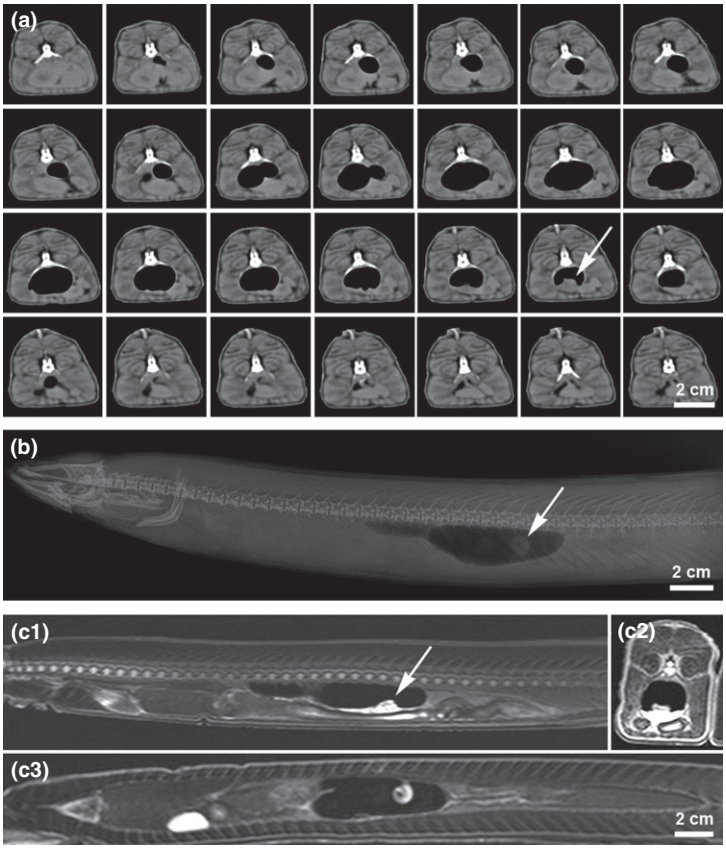

Figure 4 *Anguilla anguilla*, no. 1. (a) Computed tomography showing a clearly discernible swimbladder of a moderately infected eel; segment 20 contains a distinctly visible specimen of *Anguillicoloides crassus* (arrow). (b) Lateral radiograph of the cranial half of the same eel with a distinct radiographic shadow of a coiled worm (arrow). (c1) Lateral, (c2) transverse and (c3) dorsal T2 MRI of the same eel showing a clearly discernible swimbladder containing at least one adult worm in all three views (arrow) and fluid in the lumen.

Székely *et al.* (2004) found in their study. CT is also able to give a more accurate determination on the number of worms present and their location. None of the eels studied were so severely infected that no gas remained in their swimbladder lumen; consequently, it is not possible to comment on what the images would look like in these conditions. Székely *et al.* (2004) reported that once there is no gas within the lumen, CT is unable to provide data on wall thickness or the number and location of worms and radiographic examinations have a similar limitation (Beregi *et al.* 1998; Székely *et al.* 2004; Svékely *et al.* 2005). In this study, the barium was helpful in determining whether a gas pocket was actually within the intestine or in another structure, such as the swimbladder or pneumatic duct, particularly on the radiographs. One problem that was encountered was that results from these radiography and CT examinations correlated well with post-mortem results only in the cases of the non-infected or moderately infected eels, when large worms were present. The two mildly infected eels looked clear on the radiographs and CT images, but the post-mortem study showed small worms within the lumen of their swimbladders. MRI, which had not been used to image eel swimbladders previously, had a similar limitation; it was difficult to detect the mild infections even though this modality showed the greatest amount of detail, including the ability to see fluid and thickened fibrotic tissue. It is hypothesized that MRI would be able to show anomalies in severely infected eels, where no gas is present, which radiography and CT are unable to do. The results of this study indicate that these high-end diagnostic tools alone are not sensitive enough to detect very mild infections and may not produce the same definite diagnosis as post-mortem examination. Therefore, as mentioned by Székely *et al.* (2004), these are only recommended as complementary methods of diagnosis, primarily for research purposes.

The severity grade of infection developed by Beregi *et al.* (1998) correlated well with the SDI established by Lefebvre *et al.* (2002), but the latter one was simpler to assess, which was the aim of this index. The LRI results obtained in this

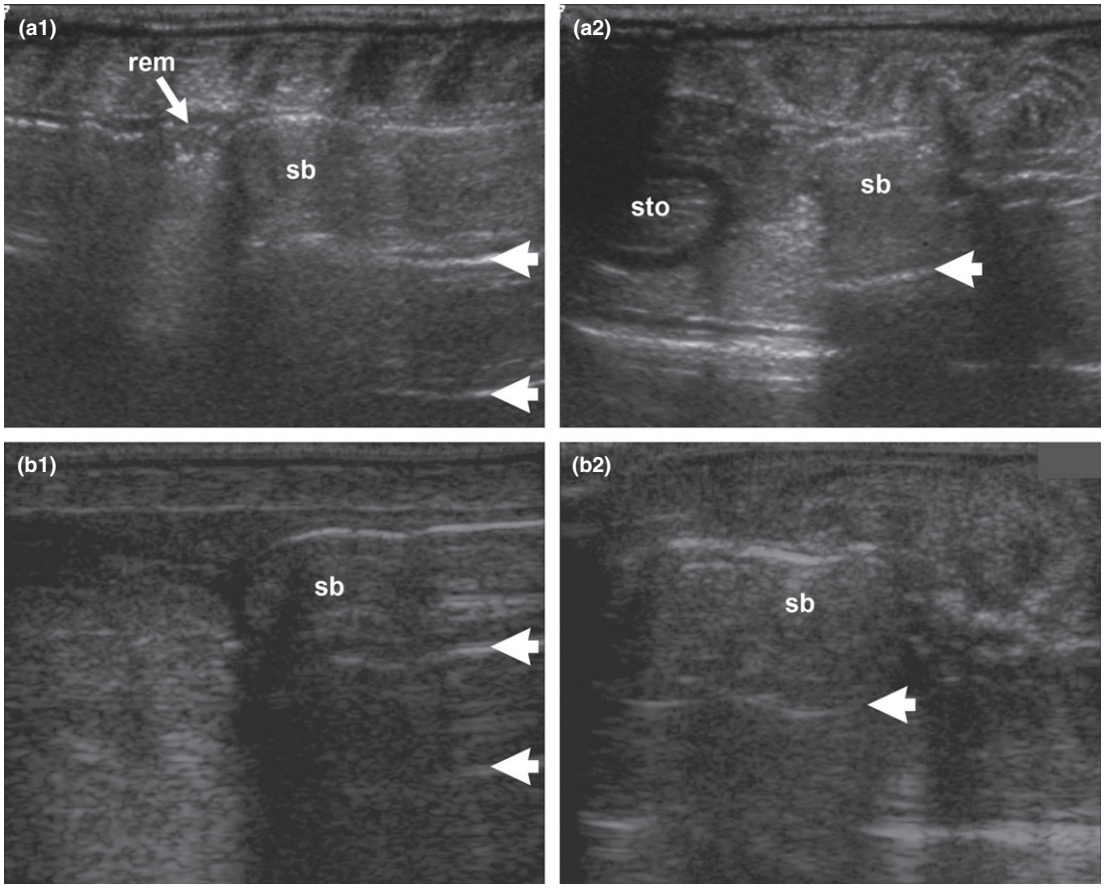

Figure 5 *Anguilla anguilla*, no. 1. (a1) Longitudinal and (a2) transverse high-end ultrasonic images of halfway through the swimbladder in Fig. 4 taken with a 14 MHz linear transducer, showing the swimbladder (sb) and stomach (sto) with reverberation artefacts (short arrows). (b1) Longitudinal and (b2) transverse low-end ultrasonic images of the same swimbladder taken with a 5 MHz linear transducer showing the swimbladder (sb) with reverberation artefacts (arrow heads).

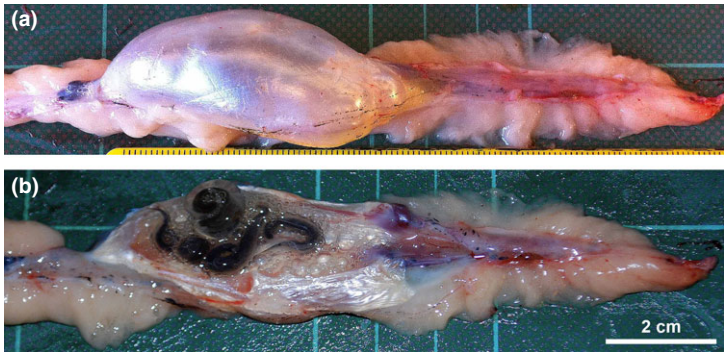

Figure 6 *Anguilla anguilla*, no. 1. (a) Unopened and (b) opened swimbladders dissected from eel in Fig. 4. Wall is opaque and thickened, the caudal end is atrophied(right image side), and the lumen is filled with worms (arrow) and some exudate.

study did not appear to follow the presumption that the smallest ratio belonged to the eels with the most severely damaged swimbladders (Lefebvre *et al.* 2011), although this may be skewed by the fact that none of the eels were severely infected.

The surprising discovery of *A. crassus* within the Loch Lomond catchment, thought to be parasite free, during the preliminary work-up to this study shows how widespread this parasite has become and how easily it establishes itself in new niches. A similar pattern has been seen in other river

Table 3 Preliminary imaging results showing length ratio index, swimbladder degenerative index, number of adult *A. crassus* within the lumen, and the severity grade of infection observed on post-mortem, radiographic, CT and MRI examinations

Number	Body length (mm)	Swimbladder length (mm)	LRI	SDI (out of 6)	Number of worms in lumen	Post-mortem Severity Grade (out of 5)	Radiography severity grade (out of 5)	CT severity grade (out of 5)	MRI severity grade (out of 5)
1	733	92	0.13	4	7	3	2	2	3
2	730	95	0.13	3	1	3	3	2	2
3	690	82	0.12	1	1	2	1	1	1
4	660	87	0.13	2	3	2	1	1	1
5	565	66	0.12	0	0	1	1	1	1

Table 4 Post-mortem results of the eels in the follow-up ultrasonic examinations showing length ratio index, swimbladder degenerative index, number of adult *A. crassus* within the lumen and the severity grade of infection observed

Number	Body length (mm)	Swimbladder length (mm)	LRI	SDI (out of 6)	Number of worms in lumen	Post-mortem severity grade (out of 5)
6	441	21	0.05	0	0	1
7	536	42	0.08	0	0	1
8	392	32	0.08	1	1	3
9	516	52	0.10	0	0	1
10	502	52	0.10	0	0	1
11	672	75	0.11	1	0	1
12	471	58	0.12	0	0	1
13	550	52	0.09	3	1	2
14	491	45	0.09	4	7	3
15	406	56	0.14	0	0	1
16	522	67	0.13	3	9	3
17	349	41	0.12	2	4	3
18	360	49	0.14	0	0	1
19	393	56	0.14	3	6	2

systems. Río Esva in north-western Spain, for example, has had few anthropogenic alterations and yet even in this nearly pristine river, there is the presence of *A. crassus* (Costa-Dias *et al.* 2010). The spread of this parasite is not solely due to human behaviour and may be attributed to the migration of intermediate, paratenic or definitive hosts, or displacement of infected eels by predators (Kirk 2003).

Kirk *et al.* (2000b) state that yellow eels may live in fresh or coastal waters for up to 27 years (Naismith & Knights 1993) before migrating and commencing gonadal differentiation; thus, the full impact of *A. crassus* is unknown, and it is therefore fundamental to develop new ways to monitor this parasite's progress. One possibility is to use a combination of tools as suggested by Lefebvre *et al.* (2011), where they propose to compute the LRI from radio-diagnostic images. The major issue with this idea is that factors other than *A. crassus* infection may affect swimbladder measurements. Also, measuring the length on radiographs relies on the contrast provided by gas within the swimbladder lumen; hence, in mildly or non-infected cases length measurements can be considered to be accurate as the whole swimbladder is filled with gas. In more severe infections, when the swimbladder is partially gas filled or completely fibrotic, length measurements cannot be accurate because it is not known whether the gas shadow seen on the radiograph corresponds to the entire length of the swimbladder. This was the main issue found when measuring lengths of organs from the images acquired in this study.

In terrestrial animals, faecal examination is one of the most common ways to detect parasites whose eggs are released through the gastrointestinal tract; this could also be used in eels. Another possible development would be a molecular-based detection technique such as the one that has been developed by Jefferies, Morgan & Shaw (2009) for the detection of the nematode *Angiostrongylus vasorum* in this parasite's definitive (canids) and intermediate (molluscs) hosts. These authors developed a real-time PCR assay that is capable of detecting first stage larvae in canine blood and faeces and detecting the third larval stage from one of this parasite's intermediate hosts, the snail,

Biomphalaria glabrata. Developing a similar assay for *A. crassus* in the eel or in an intermediate host could be the next step in monitoring this parasite in the wild. These tests have the definite advantage of lowering the limit of detection that other diagnostic tests, such as imaging, have. The other advantage is that if the larval stage in the intermediate host could be detected, the eels would not need to be killed to find out whether the parasite is present in a certain waterway. However, this would be difficult to use in the field.

In conclusion, ultrasound can be used to view changes in eels with moderate infections of *A. crassus*, particularly ones with worms and exudate in their swimbladder lumens. It is, however, unable to differentiate between mildly and parasite-free specimens, and more work is needed to determine what would be visible in severely affected eels. In view of the fast rate at which *A. crassus* is spreading, a sensitive test is needed to determine freedom from infection, but for the present time, diagnostic imaging cannot replace post-mortem as a definite diagnostic tool, and as such, more investigation is required.

Acknowledgements

We would like to thank the Royal (Dick) School of Veterinary Studies and Burgess Diagnostics Ltd. for their valuable time and expertise. We would also like to thank Chris Williams from the Environmental Agency and Colin Adams from the Scottish Centre for Ecology and the Natural Environment for providing the eels. And finally, we would like to thank Denny Conway for the photography and Kevin Erickson for helping out with post-mortems.

References

van Banning P. & Haenen O.L.M. (1990) Effect of the swimbladder nematode *Anguillicola crassus* in wild and farmed eel, *Anguilla anguilla*. In: *Pathology in Marine Science* (ed. by Perkins F.O. & Cheng T.C.), pp. 317–330. Academic Press, New York.

Beregi A., Molnár K., Békési L. & Székely C. (1998) Radiodiagnostic method for studying swimbladder inflammation caused by *Anguillicola crassus* (Nematoda: Dracunculoidea). *Diseases of Aquatic Organsims* **34**, 155–160.

Cartee R.E. (1995) The physics of ultrasound. In: *Practical Veterinary Ultrasound* (ed. by Cartree R.E.), pp. 1–8. Williams & Wilkins, Philadelphia.

CITES (2011) *Convention on International Trade in Endangered Species of Wild Fauna and Flora*. Appendices I, II and III. International Environment House, Geneva. Available at: http://www.cites.org/eng/app/E-Apr27.pdf (last accessed 4 July 2011)

Costa-Dias S., Dias E., Lobón-Cerviá J., Antunes C. & Coimbra J. (2010) Infection by *Anguillicoloides crassus* in a riverine stock of European eel, *Anguilla anguilla*. *Fisheries Management and Ecology* **17**, 485–492.

De Charleroy D., Grisez L., Thomas K., Belpaire C. & Ollevier F. (1990) The life cycle of *Anguillicola crassus*. *Diseases of Aquatic Organisms* **8**, 77–84.

Dekker W. (2003) Status of the European eel stock and fisheries. In: *Eel Biology* (ed. by Aida K., Tsukamoto K. & Yamaudi K.) pp. 237–254. Springer-Verlag, Tokyo.

Haenen O.L.M., Grisez L., De Charleroy D., Belpaire C. & Ollevier F. (1989) Experimentally induced infections of European eel *Anguilla anguilla* with *Anguillicola crassus* (Nematoda, Dracunculoidea) and subsequent migration of larvae. *Diseases of Aquatic Organisms* **7**, 97–101.

Haenen O.L.M., van Banning P. & Dekker W. (1994) Infection of eel *Anguilla anguilla* (L.) and smelt *Osmerus eperlanus* (L.) with *Anguillicola crassus* (Nematoda, Dracunculoidea) in the Netherlands from 1986 to 1992. *Aquaculture* **126**, 219–229.

ICES (2010) International Council for the Exploration of the Sea. Report of the 2010 session of the Joint EIFAC/ICES Working Group on Eels. ICES CM 2010/ ACOM:18.

Jefferies R., Morgan E.R. & Shaw S.E. (2009) A SYBR green real-time PCR assay for the detection of the nematode *Angiostrongylus vasorum* in definitive and intermediate hosts. *Veterinary Parasitology* **166**, 112–118.

Kennedy C.R. (2007) The pathogenic helminth parasites of eels. *Journal of Fish Diseases* **30**, 319–334.

Kennedy C.R. & Fitch D.J. (1990) Colonization, larval survival and epidemiology of the nematode *Anguillicola crassus*, parasitic in the eel, *Anguilla anguilla*, in Britain. *Journal of Fish Biology* **36**, 117–131.

Kirk R.S. (2003) The impact of *Anguillicola crassus* on European eels. *Fisheries Management and Ecology* **10**, 385–394.

Kirk R.S., Kennedy C.R. & Lewis J.W. (2000a) Effect of salinity on hatching, survival and infectivity of *Anguillicola crassus* (Nematoda: Dracunculoidea) larvae. *Diseases of Aquatic Organisms* **40**, 211–218.

Kirk R.S., Lewis J.W. & Kennedy C.R. (2000b) Survival and transmission of *Anguillicola crassus* Kuwahara, Niimi & Itagaki, 1974 (Nematoda) in seawater eels. *Parasitology* **120**, 289–295.

Knopf K. & Mahnke M. (2004) Differences in susceptibility of the European eel (*Anguilla anguilla*) and the Japanese eel (*Anguilla japonica*) to the swim-bladder nematode *Anguillicola crassus*. *Parasitology* **129**, 491–496.

Køie M. (1991) Swimbladder nematodes (*Anguillicola* spp.) and gill monogeneans (*Pseudodactylogyrus* spp.) parasitic on the European eel (*Anguilla anguilla*). *Journal du Conseil International pour l'Exploration de la Mer* **47**, 391–398.

Lefebvre F., Contournet P. & Crivelli A.J. (2002) The health state of the eel swimbladder as a measure of parasite pressure by *Anguillicola crassus*. *Parasitology* **124**, 457–463.

Lefebvre F., Fazio G., Palstra A.P., Székely C. & Crivelli A.J. (2011) An evaluation of indices of gross pathology associated with the nematode *Anguillicoloides crassus* in eels. *Journal of Fish Diseases* **34**, 31–45.

Martin-Robichaud D.J. & Rommens M. (2001) Assessment of sex and evaluation of ovarian maturation of fish using ultrasonography. *Aquaculture Research* **32**, 113–120.

Molnár K. (1994) Formation of parasitic nodules in the swimbladder and intestinal walls of the eel *Anguilla anguilla* due to infections with larval stages of *Anguillicola crassus*. *Diseases of Aquatic Organisms* **20**, 163–170.

Molnár K., Baska F., Csaba G., Glávits R. & Székely C. (1993) Pathological and histopathological studies of the swimbladder of eels *Anguilla anguilla* infected by *Anguillicola crassus* (Nematoda: Dracunculoidea). *Diseases of Aquatic Organisms* **15**, 41–50.

Moravec F. (1996) Aquatic invertebrates (snails) as new paratenic hosts of *Anguillicola crassus* (Nematoda: Dracunculoidea) and the role of paratenic hosts in the life cycle of this parasite. *Diseases of Aquatic Organisms* **27**, 237–239.

Moravec F. & Konecny R. (1994) Some new data on the intermediate and paratenic hosts of the nematode *Anguillicola crassus* Kuwahara, Niimi et Itagaki, 1974 (Dracunculoidea), a swimbladder parasite of eels. *Folia Parasitologica* **41**, 65–70.

Moravec F. & Škoríková B. (1998) Amphibians and larvae of aquatic insects as new paratenic hosts of *Anguillicola crassus* (Nematoda: Dracunculoidea), a swimbladder parasite of eels. *Diseases of Aquatic Organisms* **34**, 217–222.

Moriarty C. & Dekker W. (1997) Management of the European Eel. *Fisheries Bulletin (Dublin)* **15**, 1–110.

Nagasawa K., Kim Y.-G. & Hirose H. (1994) *Anguillicola crassus* and *A. globiceps* (Nematoda: Dracunculoidea) parasitic in the swimbladder of eels (*Anguilla japonica* and *A. anguilla*) in East Asia: a review. *Folia Parasitologica* **41**, 127–137.

Naismith I.A. & Knights B. (1993) The distribution, density and growth of the European eel, *Anguilla anguilla*, in the freshwater catchment of the River Thames. *Journal of Fish Biology* **42**, 217–226.

Palstra A.P., Heppener D.F.M., van Ginneken V.J.T., Székely C. & van den Thillart G.E.E.J.M. (2007) Swimming performance of silver eels is severely impaired by the swimbladder parasite *Anguillicola crassus*. *Journal of Experimental Marine Biology and Ecology* **352**, 244–256.

Penninck D.G. (2002) Artifacts. In: *Small Animal Diagnostic Ultrasound*, 2nd edn (ed. by Penninck D.G.), pp. 19–29. Saunders, Philadelphia.

Sprengel G. & Lüchtenberg H. (1991) Infection by endoparasites reduces maximum swimming speed of European smelt *Osmerus eperlanus* and European eel *Anguilla anguilla*. *Diseases of Aquatic Organisms* **11**, 31–35.

Svékely C., Molnar K. & Rácz O.Z. (2005) Radiodiagnostic method for studying the dynamics of *Anguillicola crassus* (Nematoda: Dracunculoidea) infection and pathological status of the swim bladder in Lake Balaton eels. *Diseases of Aquatic Organisms* **64**, 157–164.

Székely C. (1994) Paratenic hosts for the parasitic nematode *Anguillicola crassus* in Lake Balaton, Hungary. *Diseases of Aquatic Organisms* **18**, 11–20.

Székely C., Molnár K., Müller T., Szabó A., Romvári R., Hancz C. & Bercsényi M. (2004) Comparative study of X-ray computerised tomography and conventional X-ray methods in diagnosis of swimbladder infection in eels caused by *Anguillicola crassus*. *Diseases of Aquatic Organisms* **58**, 157–164.

Taraschewski H. (2006) Hosts and parasites as aliens. *Journal of Helminthology* **80**, 99–128.

Taraschewski H., Moravec F., Lamah T. & Anders K. (1987) Distribution and morphology of two helminths recently introduced into European eel populations: *Anguillicola crassus* (Nematoda, Dracunculoidea) and *Paratenuisentis ambiguus* (Acanthocephala, Tenuisentidae). *Diseases of Aquatic Organisms* **3**, 167–176.

Thomas K. & Ollevier F. (1992) Paratenic hosts of the swimbladder nematode *Anguillicola crassus*. *Diseases of Aquatic Organisms* **13**, 165–174.

Vogel G. (2010) Europe tries to save its eels. *Science* **329**, 505–507.

Würtz J., Taraschewski H. & Pelster B. (1996) Changes in gas composition in the swimbladder of the European eel (*Anguilla anguilla*) infected with *Anguillicola crassus* (Nematoda). *Parasitology* **112**, 233–238.

Supporting Information

Additional Supporting Information may be found in the online version of this article:

Table S1 Post-mortem measurements of the eels used in the preliminary imaging showing body length and mass, as well as liver, gall bladder, spleen, gastrointestinal, heart and swimbladder mass.

Received: 29 January 2015
Revision received: 2 April 2015
Accepted: 2 April 2015